

Overpotential Nucleation and Growth of Copper onto Polycrystalline and Single Crystal Gold Electrodes

Elizabeth Garfias-García¹, Mario Romero-Romo¹, María Teresa Ramírez-Silva²,
Manuel Palomar-Pardavé^{1,*}

¹ Universidad Autónoma Metropolitana-Azcapotzalco, Departamento de Materiales, Área Ingeniería de Materiales. Av. San Pablo #180, Col. Reynosa-Tamaulipas, C.P. 02200, México D.F.

² Universidad Autónoma Metropolitana-Iztapalapa, Departamento de Química, Av. San Rafael Atlixco #186, Col. Vicentina, C.P. 09340, México, D.F.

*E-mail: mepp@correo.azc.uam.mx

Received: 26 January 2012 / Accepted: 5 March 2012 / Published: 1 April 2012

The copper electrodeposition process was studied using cyclic voltammetry and through application of potential pulses within the so called OPD zone ($E < E_{eq}$), initiating the pulse with a jump to an anodic rest potential (E_{ar}) more positive than the equilibrium potential, E_{eq} , such that the gold surface was free from copper. The deposition was carried out onto gold electrodes having different cristallinity, namely Au single crystal, Au(111), and polycrystalline Au, from an aqueous $CuSO_4$ 1 mM dissolution in 0.1 M H_2SO_4 at pH 1.0. From the analysis of the transients obtained within the overpotential region, several mechanisms were proposed to explain the rate controlling steps underlying the overall shape of the experimental deposition transients. For the single crystal electrode three contributions to the current measured became evident, which correspond to: an adsorption process, a 2D nucleation process and a 3D diffusion-limited nucleation process. For the polycrystalline electrode the processes considered taking place during 3D multiple growths were: an adsorption process, a 3D diffusion-limited growth process and a proton reduction process occurring on the growing surface of the new copper nuclei.

Keywords: Copper; Overpotential deposition; Au(111), Nucleation kinetics

1. INTRODUCTION

The electrochemical deposition process has been determining for the manufacture of diverse new materials, which have been processed under particular methods to endow them with specific

properties, considering basically the crystallographic features of the substrate and the material to be deposited [1-11]. The systems comprised several substrates and the deposition of a single or multiple layers permitted to undertake detailed studies of the surface phenomena taking place, such as: ordered adsorption, nucleation and growth, phase transformations and several others [12].

The electrodeposition of materials allows formation of thin layers, like monolayers, with the added advantage of a better kinetic control; this is expected because there is effective control over the coverage of the deposited material monolayer. It may be safely said that the frontier of electrochemistry is actively dealing with the design and manufacture of *tailor-made* materials, from the nanometric or atomic scale up to submicron sizes. In case of Cu underpotential deposition, UPD, our research group [13] has recently shown from the analysis of the experimental current density transients, that the potentiostatic formation of a full copper monolayer onto the gold electrode under UPD conditions follows the same mechanism, regardless of the crystallinity of the substrate. The mechanism involved the simultaneous presence of an adsorption process and two 2D nucleation processes, progressive and instantaneous, respectively. On consideration of aspects relative to the receiving substrate, utilization of single crystal electrodes has attracted considerable attention and aroused greater systematisation of the determining factors, such as surface crystallographic features and morphology of the substrate, on the deposition process and the properties of the deposit resulting thereby [13-16]. The polycrystalline electrodes naturally exhibit rather a complicated nature as they possess a wider variety of surface crystallographic orientations, a finite extension of grain boundaries, and a limited variety of lattice defects and their uncertain energy configuration, all of which are likely to play a role during the nucleation stages. These features compound a panorama worthy of a comparative study respect to the single crystal deposition experiments. Moreover, we have also shown that the formation of a Cu monolayer plays a role on the bulk deposit formed at overpotential (OPD) due to 3D growth when single crystal electrodes are used [14,16].

The potentiostatic electrochemical method has proved to be most appropriate to study such kind of interfacial phenomena for several electrochemical phase formation processes, namely: metals deposition [1-4,6,18-30], conducting polymers electrosynthesis [5,7-11], surfactants condensation on polarized surfaces [17], anodic formation of passive layers [31,32]; however, they have been particularly useful to study copper electrodeposition [13-16,19]. The analysis of the temporal response of the current passing through an electrode under a given imposed potential within the framework of various theoretical formalisms, allows the determination of the dimensionality of the resulting deposit, of the rate limiting step, and a limited variety of other electrodeposition kinetic parameters. In view of the aforementioned, the present work aims to study by means of the potentiostatic technique, the initial steps of the formation and growth of copper nuclei onto a gold single crystal, Au(111), and onto polycrystalline gold.

2. EXPERIMENTAL

The experimental measurements were carried out using a typical three-electrode cell with an inert nitrogen atmosphere over the electrolyte; the working electrodes consisted of a 200 nm thick gold

layer vacuum-deposited over heat-resisting glass (Berlin Glass) with a (111) crystallographic surface orientation, and a polycrystalline gold disc as the tip of rotating disc electrode BAS, having 0.707 cm^2 exposed area. The counter electrode was a Pt wire and the reference electrode was the saturated mercury sulphate electrode, $\text{Hg}/\text{Hg}_2\text{SO}_4\text{-K}_2\text{SO}_4$ (SSE), to which all potentials reported in this work are referred. All reagents used were suprapure grade from Merck. The copper electrodeposits onto the gold electrodes were achieved applying potentiostatic current transients to 1 mM CuSO_4 solutions in H_2SO_4 0.1 M at pH 1, previously deaerated with flowing nitrogen during 20 minutes. The Millipore deionised water used to prepare the dissolutions had $18\text{ M}\Omega\cdot\text{cm}^{-1}$ resistivity. Special care was exerted with cleansing the containers and with handling other ancillary materials, but in particular with the single crystal substrates as they are particularly sensitive to contaminants, even at very low concentrations. Before each measurement, the working electrode was annealed with the aid of a hydrogen flame approximately for 30 seconds till it reached a light red colour and cooled afterwards under a hydrogen stream. The polycrystalline gold electrode was carefully polished with 0.5 and $0.1\ \mu\text{m}$ alumina particle size suspensions.

The studies of the nucleation process have been carried out using potentiostatic single pulses to effect copper electrodeposition within the overpotential region. The procedure applied was as follows: in order to ensure that the gold surface was free from copper atoms [13,14], a potential of 0.1 mV vs. SSE (E_{ar}) was applied to the working electrode before it entered into contact with the Cu(II) solution (CuSO_4 1 mM and H_2SO_4 0.1 M , pH = 1.0). Then, potential pulses (E), in this case smaller or equal to the system's equilibrium potential (E_{eq}), were imposed to the electrode surface in the so called OPD region. Determination of each OPD region was based upon the results obtained by means of cyclic voltammetry. The corresponding current transients were recorded. The cyclic voltammograms were obtained in the system: gold electrode / CuSO_4 1 mM , 0.1 M of H_2SO_4 (at pH 1). The potential scans started at 0.1 V towards the negative direction at 15 mV s^{-1} scan rate.

3. RESULTS AND DISCUSSION

3.1. Potentiodynamic study

Figure 1 shows the cyclic voltammograms obtained in the 1 mM CuSO_4 aqueous solution with $0.1\text{ M H}_2\text{SO}_4$ at pH 1 for the substrates stated. For the single crystal electrode, the potential scan initiated at 0.1 V in the negative direction and was inverted at -0.54 V , which is a potential value more negative than the equilibrium potential for the $\text{Cu(II)}/\text{Cu(0)}$ [13,14]. Figure 1(a) shows the set of characteristic peaks associated to both the UPD and OPD copper deposit onto the gold single crystal electrode: peaks A, B and A', B', refer to metal deposition and its dissolution, respectively. Similarly, peaks C and C', correspond to identical processes that must be associated to the OPD regime [14]. It should be noted that in the case of the polycrystalline electrode the overpotential necessary to initiate the copper reduction process was approximately 300 mV more negative than that for the metal deposition onto the single crystal surface. Notwithstanding, the current involved is only slightly larger compared to that for the polycrystalline electrode. Further, the voltammetry traces for both kinds of

electrodes crossed over when the scans were reversed at the potential limit selected, well into the OPD zone, which indicates the initiation of a 3D nucleation process.

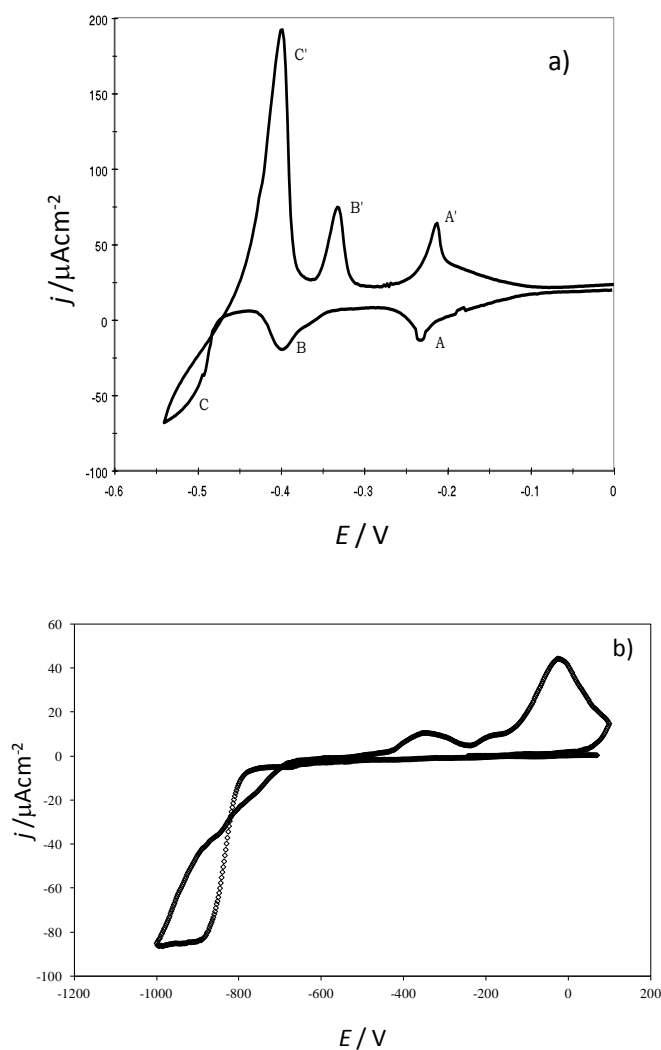


Figure 1. Cyclic voltammograms for copper electrodeposition onto (a) Gold single crystal and (b) Polycrystalline gold from 1 mM CuSO_4 aqueous solution and 0.1 M H_2SO_4 at pH 1. In both cases, the potential scan initiated at 0.1 V in the negative direction at 15 mV s^{-1} scan rate.

3.2. Potentiostatic current transients

Figure 2 shows two typical potentiostatic current transients obtained during OPD copper deposition over the two substrates used, starting with a surface free from copper ad-atoms ($E_{ar} = 0.1 \text{ V}$). From the comparison of the transients registered, it can be noted that the OPD deposit on gold displays various features derived from the substrate's crystallography. Both potentiostatic current transients, Figures 2(a) and 2(b) revealed that regardless of the kind of electrode used, the current density (j) decreased as a function of elapsing time, right from the start of the transient, though only for a brief period before it rose again. Further, the said current decay times are noticeably different for

both electrodes, the Au single crystal and the polycrystalline, namely, less than half a second and about two seconds, respectively.

After the current density fall, zone I, of the single crystal electrode, Figure 2(a) there appeared two maxima (II and III), while for the polycrystalline electrode there was only one maximum (II). Given the features of the copper-onto-gold deposition at overpotential conditions, there seems to be different processes occurring as a function of the structure of the underlying gold surface.

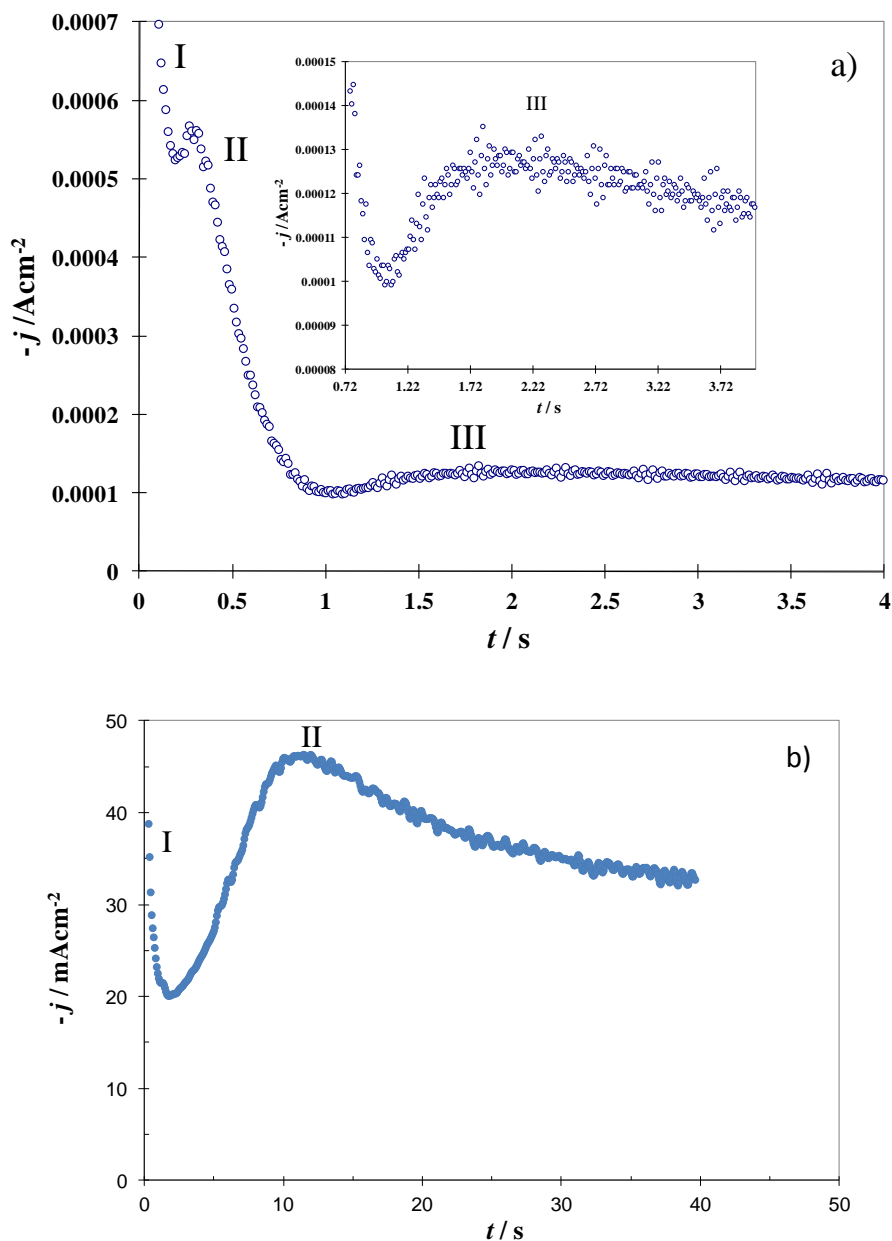


Figure 2. Typical current density transients obtained during the OPD deposition of copper onto gold, (a) single crystal and (b) polycrystalline, from a 1 mM CuSO_4 aqueous solution and 0.1 M H_2SO_4 and pH 1. The potentials used were -0.5 V (a) and -0.8 V vs. SSE (b). The Ear was 0.1 V vs. SSE for both cases. The inset in Figure 2(a) is a zoom of the region pertaining to the current density maximum denoted as III.

3.2.1 Copper OPD onto Au(111)

The features observed in the transients plotted in Figure 2(a) have been adequately described by Palomar-Pardavé *et al.* [14], see equation 1. In this case, the complete transient can be explained in terms of three coupled processes taking place simultaneously, as described in the following: Adsorption process (region I), instantaneous 2D nucleation (region II) and 3D diffusion-limited nucleation (region III). Figure 3 shows the result of the non-linear fitting of the model previously proposed to the experimental data recorded in the current transient shown in Figure 2(a) [14]. The rather close fitting of the theoretical plots can be ascribed to 2D and 3D processes occurring, which suggest that the initiation of 3D nuclei formation takes place before the 2D monolayer has been completed.

$$j(t) = j_{AD}(t) + j_{2Di-LI}(t) + j_{3D-DC}(t) \quad (1)$$

Where j_{AD} is the contribution due to adsorption or double layer charging, j_{2Di-LI} is the contribution due to an instantaneous 2D nucleation process limited by the incorporation of ad-atoms and j_{3D-DC} is related with 3D nucleation limited by the diffusion of the electroactive species.

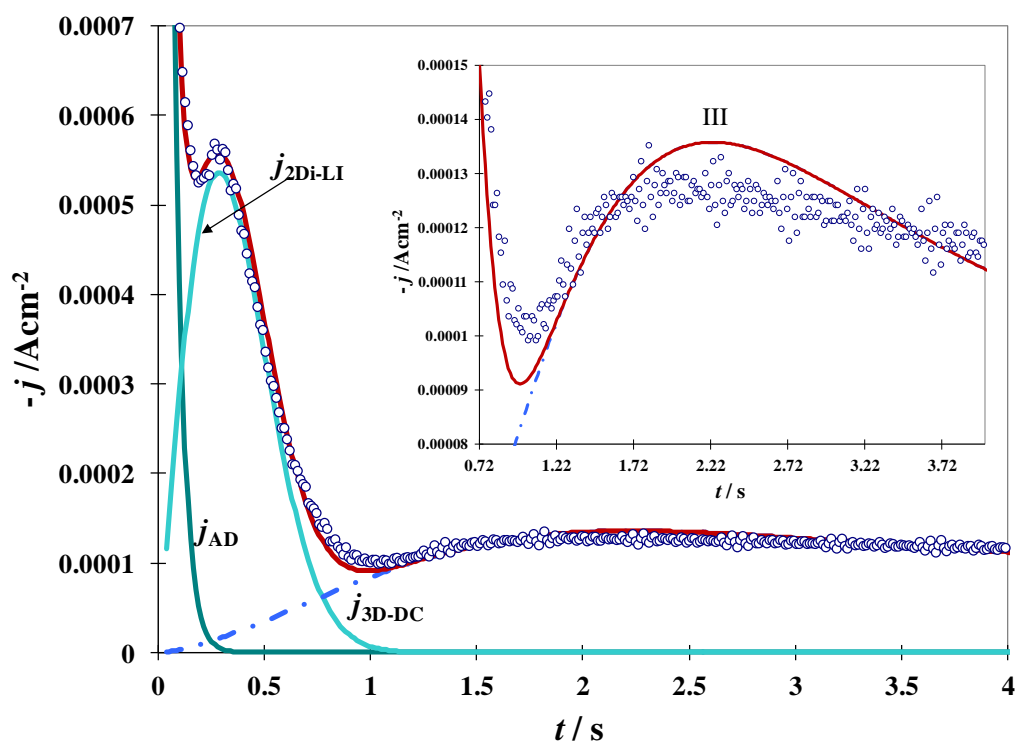


Figure 3. Comparison between the data from the experimental current transient (○○○) obtained at -0.5 V vs. SSE and a theoretical transient (continues red line) obtained as a result of the non-linear fitting procedure of equation (1), see more details in [14], to the experimental data. The individual contributions to the overall current are also shown. The inset shows a zoom of the zone III.

3.2.2 Copper OPD onto polycrystalline Au.

The previous analysis clearly demonstrated that for a single crystal gold substrate electrode there was a monolayer formed which was followed by a diffusion-limited 3D growth process (see Figure 3). However, there exists a significant difference between the transients obtained for the polycrystalline substrate as compared to the single crystal substrate, a fact which is easily adverted from a comparison of the transients in Figure 2. Figure 4 shows a family of potentiostatic transients recorded during the copper OPD on polycrystalline gold. From the observation of the transients it can be said rightly that they share common features for the 3D diffusion-limited nucleation [1-3]. It should be noted that as the potential becomes more negative, the maxima in the plots shifted toward shorter times displaying also greater current density.

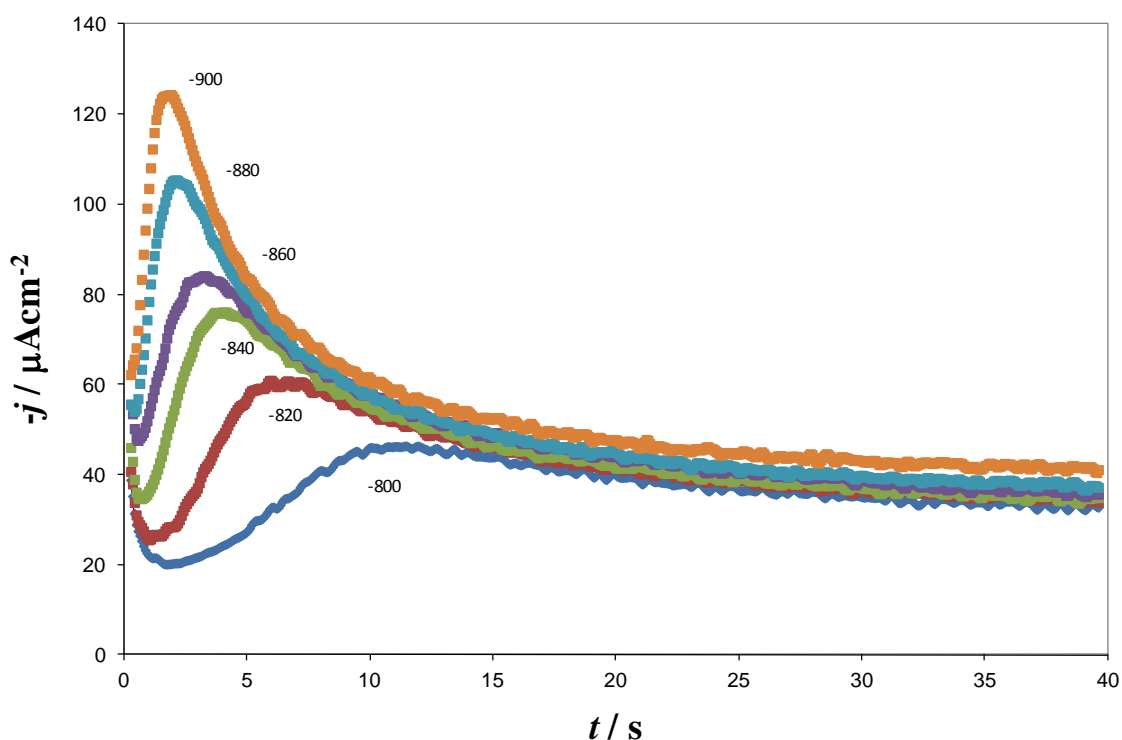


Figure 4. Potentiostatic current density transients recorded during deposition of copper OPD onto polycrystalline gold, from an aqueous dissolution containing 1 mM CuSO_4 and 0.1 M H_2SO_4 at pH 1. The applied potentials are individually indicated for each plot expressed in mV. The Ear was 0.1 mV for all cases.

On consideration of the aforementioned results, it becomes desirable to analyze the resulting transients making use of a model recently proposed by Heerman and Tarallo [3] for multiple 3D diffusion-limited nucleation processes. Figure 5 shows the comparison between the experimental and the theoretical transients derived from non-linear fitting of the experimental data to the model proposed by the said authors, thus using equation (2).

$$j(t) = zDFDc(\pi Dt)^{-1/2} \frac{\Phi}{\Theta} (1 - \exp[-\pi k N_0 Dt \Theta]) \tag{2}$$

where $\Phi \equiv \Phi[(At)^{1/2}]$, is related to the Dawson-type integral given by:

$$\Phi = 1 - \frac{\exp(-At)}{(At)^{1/2}} \int_0^{(At)^{1/2}} \exp \lambda^2 d\lambda \tag{3}$$

where $k = (8\pi M c / \rho)^{1/2}$ and $\Theta \equiv \Theta[At]$ are given by:

$$\Theta = 1 - [1 - \exp(-At)] / At \tag{4}$$

In equations (2) – (4), j is the current density, t is the time, D is the diffusion coefficient, A is the nucleation rate, N_0 is the density of active sites, c is the concentration, M and ρ are the molecular weight and the density of the deposit, respectively, zF is the charge associated to the reduction of the metal ion.

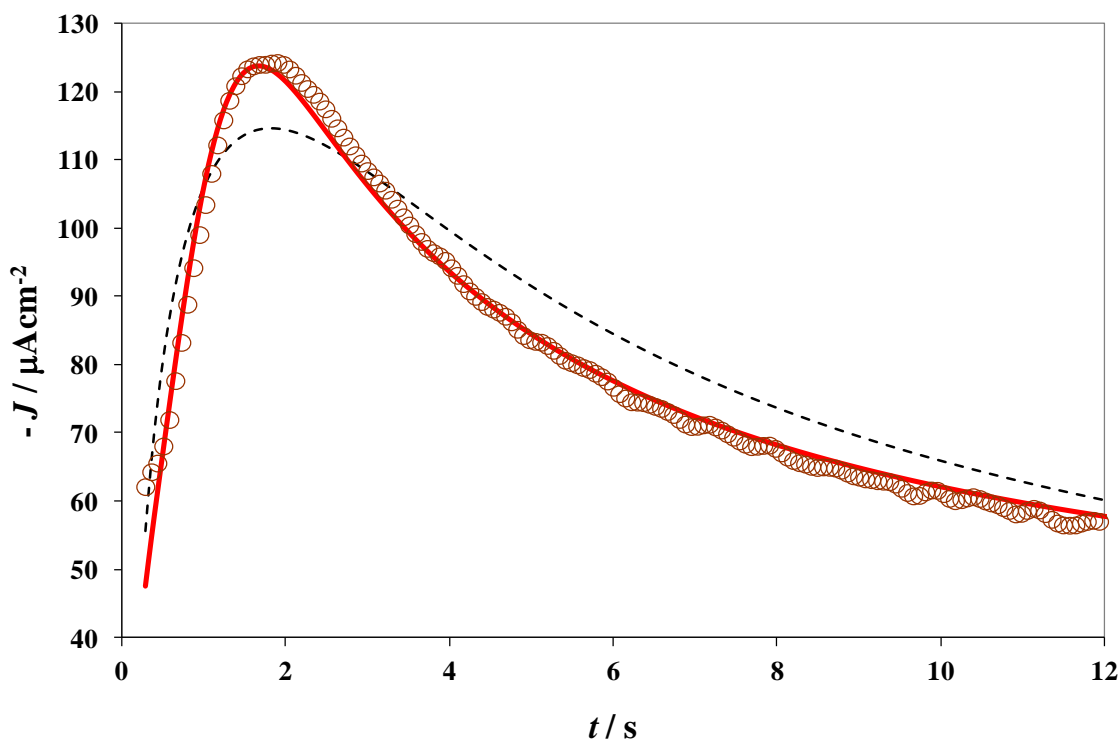


Figure 5. Comparison between the experimental potentiostatic transient (OOO) obtained during the massive deposit of Cu onto polycrystalline Au, with -0.90 V as the applied potential, from the aqueous dissolution containing 1 mM CuSO₄ and 0.1 M H₂SO₄ at pH 1. One theoretical transient (dashed line) is described by equation (2), the other theoretical transient (red line) is described by equation (5). Both theoretical transients were obtained by non-linear fitting of the respective equations to the experimental data.

From examination of Figure 5, it becomes evident that the non-linear fitting of equation (2) to the experimental data can be described as poor. In order to produce a better description of the transients, other factors need to be taken into consideration to compose a better alternative. In particular, it should be noted that the massive copper deposit onto the polycrystalline gold substrate requires a greater overpotential (approximately 300 mV) as compared to that for the Au(111) electrode. This situation may well imply that another reaction is simultaneously taking place within the system, such as the proton reduction (PR), and that this has been increasingly gaining kinetic importance. Palomar-Pardavé *et al.* [18] have proposed another model which is capable of describing the potentiostatic transients obtained during metal electrodeposition processes that occur along the PR. For that matter, the said authors proposed the equation put forward by Scharifker *et al.* [1], or Heerman and Tarallo model [3] to describe the contribution due to a 3D nucleation process limited by the mass transfer reaction. In this work, a third contribution due to an adsorption process ($j_{ad}(t)$) is proposed in order to analyze current density transients as those reported in Figure 4. The mathematical modification is represented by the following equation (5):

$$j(t) = j_{Ad}(t) + j_{PR}(t) + j_{3D-DC}(t) \tag{5}$$

where

$$j_{ad} = K_1 \exp(-K_2 t) \tag{6}$$

with $K_1 = \frac{E}{R_s}$, $K_2 = \frac{1}{R_s C}$

In this case E represents the applied potential throughout the perturbations, R_s is the solution's resistance, C the double layer capacitance.

$$j_{PR}(t) = P_1 S(t) \tag{7}$$

with $P_1 = z_{PR} F k_{PR}$, where $z_{PR} F$ is the molar charge transferred during the proton reduction process, k_{PR} is the rate constant of the proton reduction reaction and $S(t) = (2c_0 M / \pi \rho)^{1/2} \theta(t)$ is the fractional surface area of electrodeposited copper:

$$S(t) = \left(\frac{2c_0 M}{\pi \rho} \right)^{1/2} \left\{ 1 - \exp \left\{ -P_2 \left[t - \frac{1 - \exp(-P_3 t)}{P_3} \right] \right\} \right\} \tag{8}$$

where c_0 is the concentration of the metal ion in the bulk solution, ρ is the density of the deposit, M is its molar mass, $P_2 = N_0 \pi k D$, $k = (8 \pi c_0 / \rho)^{1/2}$ and $P_3 = A$, with N_0 and A being the number density of active sites for nucleation on the electrode surface and the rate of nucleation, respectively. The current associated to the contribution due to the copper reduction process (j_{3D-dc}), on the other hand, is given by [3]:

$$j_{3D-dc}(t) = P_4 t^{-1/2} \theta(t) \tag{9}$$

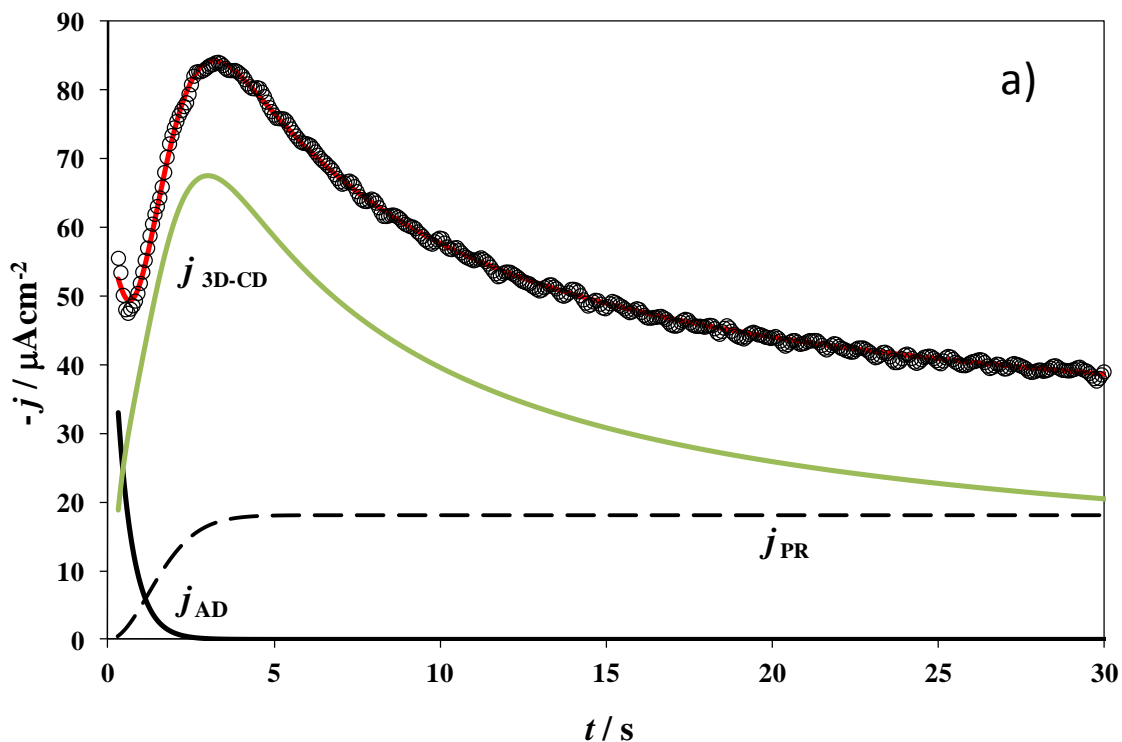
where $P_4 = \frac{2FD^{1/2}c_0}{\pi^{1/2}}$ and $\theta(t) = \left\{ 1 - \exp \left\{ -P_2 \left[t - \frac{1 - \exp(-P_3 t)}{P_3} \right] \right\} \right\}$. The current due to the overall process (j_{total}) is the sum of all contributions $j_{Ad} + j_{PR} + j_{3D-dc}$ and is hence given by

$$j_{total}(t) = \left(P_1^* + P_4 t^{-1/2} \right) \left(1 - \exp \left\{ -P_2 \left[t - \frac{1 - \exp(-P_3 t)}{P_3} \right] \right\} \right) + K_1 \exp(-K_2 t) \tag{10}$$

where $P_1^* = P_1 \left(\frac{2c_0 M}{\pi \rho} \right)^{1/2}$

It must be added that Figure 5 also shows the trace of the transient generated by non-linear fitting of equation (5) to the experimental data, but it is worthy to underline that the use of the said equation has provided a more accurate description of the deposition phenomena included in the transient.

It is pertinent to clarify that the transients shown in Figure 4, obtained at lower potentials, also involve at short times, a contribution that can be represented by the charge of the double layer. Now, when this contribution is added to equation (5), the representation of the resulting transients at low overpotentials can be adequately performed, as seen in Figure 6.



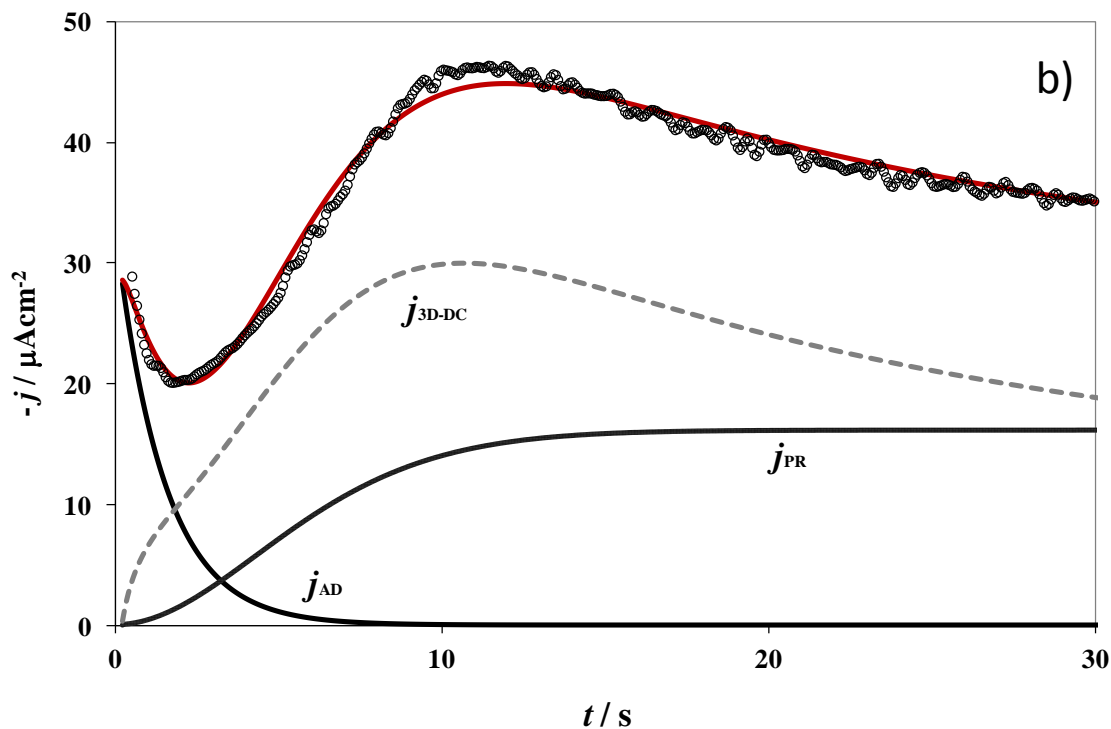


Figure 6. Comparison between the experimental potentiostatic current transient (○○○) obtained during copper electrodeposition onto a polycrystalline gold electrode, from an aqueous dissolution containing 1 mM CuSO_4 and 0.1 M H_2SO_4 at pH 1, for an applied potential of: (a) -0.86 V and (b) -0.80, and a theoretical transient (continuous red line) obtained by non-linear fitting of the experimental data to equation (5). Also, the three contributions to the overall current density are displayed individually: an adsorption process or double layer charge (j_{AD}), a 3D diffusion-limited nucleation process (j_{3D-DC}) and a hydrogen reduction process (j_{PR}).

Furthermore, in Figure 6 the three main contributions have been made clearly distinguishable to highlight that the overall growth mechanism propounded involves the simultaneous interaction of an adsorption process (double layer charge) together with multiple nucleation and diffusion limited 3D growth, the latter occurring concomitantly with protons reduction.

4. CONCLUSIONS

The copper electrochemical nucleation process in the OPD region has been described qualitatively and quantitatively on gold substrates having different crystallinity. It became evident that for the Au(111) single crystal the deposition involved three processes simultaneously contributing to the construction of the deposit, namely, double layer charging, instantaneous 2D nucleation and diffusion-limited 3D nucleation. However, for the polycrystalline electrode, the copper nucleation process required an applied overpotential of at least 300 mV greater as compared to that necessary for the single crystal Au(111). The said situation favoured the occurrence of the faradaic concomitant

hydrogen evolution reaction, though keeping in mind that the model proposed herein has described appropriately the overall shape of the experimental data transients.

ACKNOWLEDGEMENTS

The authors gratefully acknowledge the SNI for the distinction of their membership and the stipend received. M.R.R. and M.P.P. would like to thank CONACYT for project 22610714. Also, the authors wish to express their gratitude to Departamento de Materiales at UAMA for the support given through Projects DM.AIM.01-07.

References

1. B.R. Scharifker, J. Mostany, M. Palomar-Pardavé, I. González. *J. Electrochem. Soc.* 146 (1999) 1005.
2. M. Sluyters-Rehbach, J. H. O. J. Wijenberg, E. Bosco and J. H. Sluyters, *J. Electroanal. Chem.*, 283 (1990) 35.
3. L. Hearman and A. Tarallo. *Electrochem. Comm.* 2 (2000) 85.
4. M. Y Abyaneh, M. Fleischmann. *J. Electrochem. Soc.* 138 (1991) 2491.
5. G.A. Álvarez-Romero, E. Garfias-García, M.T. Ramírez-Silva, C. Galán-Vidal, M. Romero-Romo, M. Palomar-Pardavé. *Appl. Surf. Sci.*, 252 (2006) 5783.
6. L.H. Mendoza-Huizar, J. Robles, M. Palomar-Pardavé, *J. Electroanal. Chem.* 521 (2002) 95.
7. J.A Cobos-Murcia, L. Galicia, A. Rojas-Hernández, M.T. Ramírez-Silva, R. Álvarez-Bustamante, M. Romero-Romo, G. Rosquete-Pina, M. Palomar-Pardavé, *Polymer*, 46 (2005) 9053.
8. E. Garfias-García, M. Romero-Romo, M.T. Ramírez-Silva, J. Morales, M. Palomar-Pardavé, *J. Electroanal Chem.* 613 (2008) 67.
9. T. de J. Licona-Sánchez, G. A. Álvarez-Romero, L. H. Mendoza-Huizar, C. A. Galán-Vidal, M. Palomar-Pardavé, M. Romero-Romo, H. Herrera-Hernández, J. Uruchurtu, J. M. Juárez-García, *J. Phys. Chem. B*, 114 (2010) 9737.
10. E. Garfias-García, M. Romero-Romo, M. T. Ramírez-Silva, J. Morales, M. Palomar-Pardavé, *Int. J. Electrochem. Sci.*, 5 (2010) 763.
11. T. de J. Licona-Sánchez, G. A. Álvarez-Romero, M. Palomar-Pardavé, C. A. Galán-Vidal, M. E. Páez-Hernández, M. T. Ramírez Silva, M. Romero-Romo, *Int. J. Electrochem. Sci.*, 6 (2011) 1537.
12. A. Milchev, *Electrocrystallization: Fundamentals of Nucleation and Growth*, Kluwer Academic Publishers, The Netherlands, 2002.
13. M. Palomar-Pardavé, E. Garfias-García, M. Romero-Romo, M.T. Ramírez-Silva, N. Batina. *Electrochim. Acta* 56 (2011) 10083.
14. M. Palomar Pardavé, I. González and N. Batina *J. Phys. Chem. B* 104 (2000) 3545.
15. A. Martínez-Ruiz, M. Palomar-Pardavé, J. Valenzuela-Benavides, M.H. Farias, N. Batina, *J. Phys. Chem. B* 107 (2003) 11660.
16. A. Martínez-Ruiz, M. Palomar-Pardavé, N. Batina *Electrochim. Acta* 53 (2008) 2115–2120.
17. E. Sánchez-Rivera, V. Vital-Vaquier, M. Romero-Romo, M. Palomar-Pardavé, M.T. Ramírez-Silva, *J. Electrochem. Soc.* 151 (2004) C666.
18. M. Palomar-Pardavé, B.R. Scharifker, E.M. Arce, M. Romero-Romo, *Electrochim. Acta* 50 (2005) 4736.
19. A. Milchev, T. Zapryanova, *Electrochim. Acta* 51 (2006) 2926.
20. A. Milchev, T. Zapryanova, *Electrochim. Acta* 51 (2006) 4916.
21. T. Zapryanova, A. Hrussanova, A. Milchev, *J. Electroanal. Chem.* 600 (2007) 311.
22. M.E. Hyde, R.G. Compton, *J. Electroanal. Chem.* 549 (2003) 1.

23. B.R. Scharifker, J. Mostany, in: A.J. Bard, M. Stratmann (Eds.), *Encyclopedia of Electrochemistry*, vol. 2, Wiley/VCH, Weinheim, 2003, p. 512.
24. E. Barrera, M. Palomar Pardavé, N. Batina, I. González, *J. Electrochem. Soc.* 147 (2000) 1787.
25. M. Palomar-Pardavé, I. González, A.B. Soto, E.M. Arce, *J. Electroanal. Chem.* 443 (1998) 125.
26. L.H. Mendoza-Huizar, J. Robles, M. Palomar-Pardavé, *J. Electroanal. Chem.* 545 (2003) 39.
27. M. Arbib, B. Zhang, V. Lazarov, D. Stoychev, A. Milchev, C. Buess-Herman, *J. Electroanal. Chem.* 510 (2001) 67.
28. C. Ramírez, E.M. Arce, M. Romero-Romo M. Palomar-Pardavé, *Solid State Ionics* 169 (2004) 5.
29. M.H. Hölzle, U. Retter, D.M. Kolb, *J. Electroanal. Chem.* 371 (1994)101.
30. M. Aguilar-Sánchez, M. Palomar-Pardavé, M. Romero-Romo, M.T. Ramírez-Silva, E. Barrera, B.R. Scharifker, *J. Electroanal. Chem.* 647 (2010) 128.
31. L. I. Espinoza-Ramos, C. Ramírez, J.M. Hallen-López, E. Arce, M. Palomar-Pardavé, M. Romero-Romo, *J. Electrochem. Soc.* 149 (2002) B543.
32. A.Hernández-Espejel, M. Palomar-Pardavé, R. Cabrera-Sierra, M. Romero-Romo, M.T. Ramírez-Silva, E.M. Arce-Estrada, *J. Phys. Chem. B* 115 (2011) 1833.